Can Diffusions Propagate?

F. Debbasch · D. Espaze · V. Foulonneau

Abstract The diffusion of relativistic particle in a fluid at equilibrium is investigated through an analytical and numerical study of the Relativistic Ornstein-Uhlenbeck process (ROUP). Contrary to expectations, the ROUP exhibits short-time propagation in physical space and only displays typical diffuse behavior at asymptotic times. The short-time propagation is understood through an analytical computation and the density profile is fitted at all times by a simple *Ansatz*. A generalization of Fick's law is finally obtained, in which the diffusion coefficient is replaced by a time-dependent metric. These results connect relativistic diffusion with gravitational horizons and geometrical flows.

Keywords Relativistic stochastic processes · Bounded velocity diffusion

1 Introduction

Transport at effectively bounded velocity is encountered in many different contexts, from astrophysics [23] and fusion plasma physics [15, 25] to metal [18, 22] and computer engineering [4], and even tumor treatment [19, 21]. Finding physically and mathematically sound models of such transport is a long standing problem of statistical physics [3, 8, 16, 17, 27]. The Relativistic Ornstein-Uhlenbeck Process (ROUP) has been introduced in 1997 [13] as the simplest possible model of relativistic particle transport and can also be used as a blueprint [8] to construct models of non-relativistic transport at bounded velocities.

The ROUP is built after the traditional, non-relativistic Langevin equation [29] and determines the stochastic phase-space trajectory of a relativistic particle diffusing in a fluid at equilibrium. The projection of this trajectory onto momentum space has been analyzed, both at short and asymptotic times [14]. The projection onto position space, however, has only been studied in the long time limit [1, 11], where bounded velocity effects cannot be captured by macroscopic equations [30], and the short-time density profile predicted by the ROUP has never been explored.

F. Debbasch (✉) · D. Espaze · V. Foulonneau
LERMA, UMR 8112, UPMC, Paris, France
e-mail: fabrice.debbasch@gmail.com

This article fills this gap by presenting the first systematic, analytical and numerical analysis of the ROUP at short and intermediate times. We consider the relativistic diffusion of particles which start their motions from some common origin point O and which are initially thermalized with the surrounding fluid. The density profile is, at short times, strikingly different from the predictions of both standard and hyperbolic diffusion models. Indeed, instead of spreading around O, most diffusing particles propagate away from O at a velocity very close to the velocity of light. As time goes, less and less particles propagate away from their initial point, and the density profile slowly tends towards the Gaussian predicted by Fick's law. We present an analytical computation which delivers an approximate analytical expression of the density profile at short-times and, thus, sheds light on the origin of the short-time propagation. We complement this analytical expression of the short-time density profile by exhibiting a simple function which fits the density profile at all times with a precision better than 3 %. We finally introduce a generalization of Fick's law which correctly describes the diffusion in physical space at all times. The diffusion coefficient is replaced by a time-dependent diffusion metric which, at any time t, tends to infinity for points at a Euclidean distance ct from O and, thus, prevents particles from being transported at supraluminal velocities. As t increases and tends to infinity, the limit distance ct also tends to infinity; the metric becomes flatter, except near ct *i.e.* near infinity, and finally tends towards the Euclidean metric over the whole space; our generalized law then degenerates into the standard Fick's law.

These results show that bounded velocity diffusions propagate at short times and can be described as diffusions in time-dependent metrics. The propagation effect is particularly striking and is surely relevant to first-passage time computations. On the purely mathematical side, our results connects bounded velocity diffusions to the general field of geometrical flows.

2 The Relativistic Ornstein-Uhlenbeck Process

The ROUP is a stochastic process which describes the diffusion of a special relativistic point mass m in a fluid at equilibrium with temperature θ_e. It is completely defined [13], in n space dimensions, by the equations of motion of the point mass in the rest frame of fluid:

$$d\mathbf{x} = \frac{\mathbf{p}}{m\gamma}dt \tag{1}$$

$$d\mathbf{p} = -\alpha\frac{\mathbf{p}}{\gamma}dt + \sqrt{2D}\,d\mathbf{B}_t, \tag{2}$$

where $\gamma = \sqrt{1 + (\frac{\mathbf{p}}{mc})^2}$ and $\mathbf{p}^2$ is the squared Euclidean norm of $\mathbf{p}$. Equation (1) is simply the definition of the relativistic n-momentum in terms of the velocity [24]. Equation (2) states that the force acting on the particle splits into two contributions. The first one is a deterministic friction $-\alpha\mathbf{p}/\gamma$, which forces the n-momentum to relax to the vanishing n-momentum of the fluid in which the particle diffuses, and the second one is a n-dimensional centered Gaussian white noise. The noise coefficient D is linked to α and θ_e by the fluctuation-dissipation relation $k_B\theta_e = D/\alpha$.

The temperature θ_e and the mass m define the thermal velocity $v_{th} = (k_B\theta_e/m)^{1/2}$; this velocity, combined with the time-scale α^{-1}, defines the length-scale $\lambda_{th} = v_{th}\alpha^{-1}$. We use these characteristic scales to define dimensionless time, position and momentum variables T, X and P by $T = \alpha t$, $\mathbf{X} = \mathbf{x}/\lambda_{th}$ and $\mathbf{P} = \mathbf{p}/(mv_{th})$. The relativistic character of the problem is traced by the quotient

$$Q = \frac{c}{v_{\text{th}}} = \left(\frac{mc^2}{k_B \theta_e}\right)^{1/2}.$$

This parameter is the dimensionless value of the light velocity c. The Galilean limit corresponds to $Q \to \infty$ and the so-called ultrarelativistic case corresponds to $Q \to 0$.

The equations of motion, being stochastic, do not generate a single trajectory from a given initial condition, but rather an infinite set of possible trajectories. The position of the particle in its phase-space $\mathbb{R}^{2n} = \{\mathbf{X}, \mathbf{P}\}$ is thus represented, for a given initial condition and value of Q, by a probability density $F_Q(T, \mathbf{X}, \mathbf{P})$ with respect to $d^n X d^n P$. This density obeys the forward Kolmogorov equation

$$\partial_T F_Q + \nabla_{\mathbf{X}} \cdot \left(\frac{\mathbf{P}}{\Gamma_Q(\mathbf{P})} F_Q\right) = \mathcal{L}_Q F_Q, \tag{3}$$

where

$$\mathcal{L}_Q F_Q = \nabla_{\mathbf{P}} \cdot \left(\frac{\mathbf{P}}{\Gamma_Q(\mathbf{P})} F\right) + \Delta_{\mathbf{P}} F_Q \tag{4}$$

and $\Gamma_Q(\mathbf{P}) = \sqrt{1 + (\mathbf{P}/Q)^2}$ is the Lorentz factor.

The Jüttner distribution [20] describing a relativistic thermal equilibrium at temperature θ_e reads simply:

$$F_Q^{\star}(\mathbf{P}) = A \exp\left(-Q^2 \Gamma_Q(\mathbf{P})\right), \tag{5}$$

where A is the normalization factor; this distribution obeys $\mathcal{L}_Q F_Q^{\star} = 0$.

The density of the process $N_Q(T, \mathbf{X})$ and the particle current density $\mathbf{J}_Q(T, \mathbf{X})$ at time T and position $\mathbf{X}$ are defined by:

$$N_Q(T, \mathbf{X}) = \int_{\mathbb{R}^n} F_Q(t, X, P) d^n P \tag{6}$$

and

$$\mathbf{J}_Q(T, \mathbf{X}) = \int_{\mathbb{R}^n} \frac{\mathbf{P}}{\Gamma_Q(\mathbf{P})} F_Q(T, \mathbf{X}, \mathbf{P}) d^n P. \tag{7}$$

They obey the continuity relation $\partial_T N_Q + \partial_{\mathbf{X}} \cdot \mathbf{J}_Q = 0$. Fick's law posits that the current density and density gradient are proportional to each other with constant coefficient. This simple assumption is not valid for the ROUP. The generalized Fick's law obeyed by the ROUP is presented in Sect. 4 below.

The spatial Fourier transform $\hat{F}_Q$ of the phase-space density F_Q is defined by
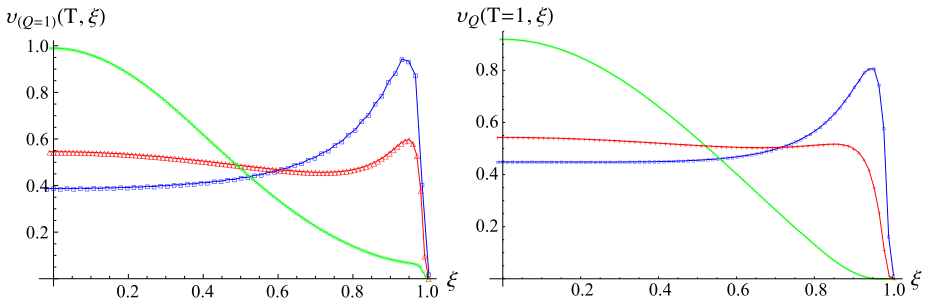
$$\hat{F}_Q(T, \mathbf{K}, \mathbf{P}) = \frac{1}{\sqrt{2\pi}} \int_{\mathbb{R}^n} F_Q(T, \mathbf{X}, \mathbf{P}) \exp(i\mathbf{K} \cdot \mathbf{X}) d^n X \tag{8}$$

and obeys:

$$\partial_T \hat{F}_Q + i\mathbf{K} \cdot \left(\frac{\mathbf{P}}{\Gamma_Q(\mathbf{P})} \hat{F}_Q\right) = \mathcal{L}_Q \hat{F}_Q. \tag{9}$$

The Fourier transform $\hat{N}_Q$ is defined in a similar manner and coincides with the integral of $\hat{F}_Q$ over P. Suppose a diffusing particle is put into the fluid at time $T = 0$ with initial position $\mathbf{X} = 0$ and initial temperature $\theta = \theta_e$. The initial condition for Eq. (3) is then

$$F_Q(T = 0, \mathbf{X}, \mathbf{P}) = \delta(\mathbf{X}) F_Q^{\star}(\mathbf{P}), \tag{10}$$

Fig. 1 Density profile and propagation. (*left*) Rescaled density-profile ν_Q against rescaled position $\xi = x/(ct)$ for $Q = 1$ and $T = 0.5$ (*blue squares*), $T = 2$ (*red triangles*) and $T = 10$ (*green circles*). (*right*) Rescaled density-profile ν_Q against rescaled position $\xi = x/(ct)$ for $T = 1$ and $Q = 1$ (*blue squares*), $Q = 1.2$ (*red triangles*) and $Q = 2$ (*green circles*)

or, in Fourier space,

$$\hat{F}_Q(T = 0, \mathbf{K}, \mathbf{P}) = \frac{1}{\sqrt{2\pi}} F_Q^\star(\mathbf{P}). \tag{11}$$

This initial condition fully determines, for each value of Q, the value of density F_Q at all times and phase-space positions. Equation (9) does not involve any derivation with respect to $\mathbf{K}$, which can thus be viewed as a simple parameter (as opposed to a fully-fledged variable with respect to which derivations are performed). Numerical simulations have been carried out by solving (9) in $n = 1$ dimension for different, regularly spaced values of K and with initial condition (11). The function F_Q has been recovered by Fast Fourier Transform and the spatial density N_Q as well as the current J_Q have been obtained from F_Q by direct numerical quadrature. All simulations have been performed with Mathematica 8. Various integration methods and limit conditions in P have been used, to ensure the robustness of numerical results.

3 The Density Profile of the ROUP

3.1 Qualitative Discussion

Since the particle is initially located at $x = 0$, the spatial density $N_Q(T, X)$ at time T and point X vanishes for $|X| > QT$ (remember Q is the dimensionless value of the light velocity c). To obtain the best visual representation of the early time evolution of the density profile, we introduce the rescaled position variable $\xi = X/QT$ and the rescaled density $\nu_Q(T, \xi) = N_Q(T, QT\xi)/(QT)$, which is normalized to unity against the measure $d\xi$. Figure 1 presents typical plots of ν_Q against ξ for different values of T and Q, supposing the particle is initially thermalized with the fluid (see Eq. (10)). At early times, the maximum of the density profile is not situated at $\xi = 0$ *i.e.* at the starting point of the diffusion, but rather at $|\xi| = \xi_Q$ where ξ_Q is time-independent and approximately equal to 0.948. This corresponds to $X_Q(T) \approx 0.948 QT$ *i.e.* $x_Q(t) \approx 0.948 ct$. This means that the diffusion, at early times, mostly propagates at velocity $\tilde{c} \approx 0.95c$. In time, a secondary maximum appears at the origin point $\xi = 0$. This secondary maximum grows and finally becomes much higher than the peaks at $\pm \xi_Q(T)$. The density profile thus gets closer and closer to the standard Gaussian $G(T, X)$ predicted by Fick's law. This can be verified by computing the norm
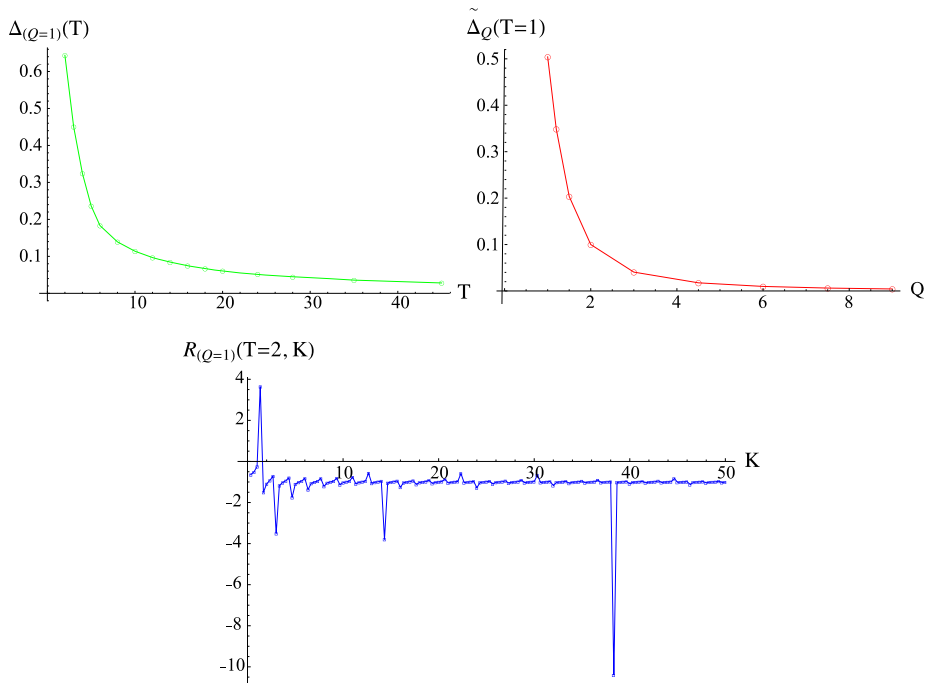
Fig. 2 Analysis of the density profile. (*top left*) Time-evolution of the absolute distance between the relativistic density profile N_Q and the Fick profile G for $Q = 1$. (*top right*) Evolution with Q of absolute distance between the relativistic density profile N_Q and the Galilean profile N_G for $T = 1$. (*bottom*) Evolution with K of the relative discrepancy between $\partial_T N_Q$ and $\square N_Q$ for $Q = 1$ and $T = 2$. The hyperbolic Cattaneo model predicts R identically vanishes

$$\Delta_Q(T) = \int_{\mathbb{R}} |N_Q(T, X) - G(T, X)| \, dX \tag{12}$$

with

$$G(T, X) = \frac{1}{\sqrt{2\pi T}} \exp\left(-\frac{X^2}{2T}\right). \tag{13}$$

Figure 2(top left) displays the time-evolution of Δ_Q for $Q = 1$ and confirms that the law of the process converges towards G, as expected from [1, 11].

Fix now an arbitrary, not necessarily large time T and consider the density profile $N_Q(T, \cdot)$ at this time. As Q tends to infinity, this density profile tends as expected towards the density profile predicted by the non-relativistic Ornstein-Uhlenbeck process [12]:

$$N_G(T, \cdot) = \frac{1}{\sqrt{2\pi \sigma_G^2(T)}} \exp\left(-\frac{X^2}{2\sigma_G^2(T)}\right) \tag{14}$$

with $\sigma_G^2(T) = (T - 1 + \exp(-T))$. This is illustrated in Fig. 2(top right), which plots the evolution with Q of the norm

$$\tilde{\Delta}_Q(T) = \int_{\mathbb{R}} |N_Q(T, X) - N_G(T, X)| \, dX \tag{15}$$

for $T = 1$. Note also that the time at which the secondary maximum appears at the origin is a decreasing function of Q and tends to zero as Q tends to infinity *i.e.* in the Galilean limit.

Let us conclude this section by showing that the spatial density of the ROUP does not obey Cattaneo's hyperbolic diffusion equation [3], which is a popular model of bounded speed transport. Cattaneo's damped wave equation reads:

$$\partial_T N = \Box_Q N = \left(\partial_{XX} - \frac{1}{Q^2} \partial_{TT} \right) N, \tag{16}$$

where $\Box_Q$ is the D'Alembert operator with velocity Q. We have computed numerically the relative discrepancy $R_Q(T)$ between $\partial_T N_Q$ and $\Box_Q N_Q$; Fig. 2(bottom) displays a typical result in Fourier space. This figure clearly displays the failure of Cattaneo's hyperbolic diffusion model to reproduce the correct density profile of the ROUP.

3.2 Analytical Computation of the Short-Time Density Profile

An approximate analytical expression for the short-time density profile presented in the previous section can be obtained by the following argument.

Consider a diffusing particle starting its motion from point O with initial impulse P_0. For sufficiently small times, the position X_T of this particle at time T varies linearly with T:

$$X_T = \frac{P_0}{\Gamma_Q(P_0)} T + O(T^2). \tag{17}$$

The probability law of X_T and, thus, the density N_Q are then entirely determined by the probability law of P_0 *i.e.* the initial momentum distribution of the particle. More precisely, X_T/T has the same probability law as the initial velocity of the particle. This law can be obtained by changing variables in the initial momentum distribution $F_Q^*(P)$. The momentum P and the velocity V of the relativistic particle are related by

$$P = \gamma_Q(V)V \tag{18}$$

where

$$\gamma_Q(V) = \frac{1}{\sqrt{1 - \frac{V^2}{Q^2}}} \tag{19}$$

is the Lorentz factor associated to the velocity V. By direct differentiation,

$$dP = \left(\gamma_Q(V) \right)^3 dV \tag{20}$$

and

$$F_Q^*(P) \, dP = f_Q^*(V) \, dV \tag{21}$$

with (see Eq. (5))

$$f_Q^*(V) = A \left(\gamma_Q(V) \right)^3 \exp \left(-Q^2 \gamma_Q(V) \right). \tag{22}$$

Replacing V by X/T in the above equations, one obtains the following approximate expression for the density N_Q at short times:

$$N_Q(T, X) \approx \frac{A}{T} \left(\gamma_Q \left(\frac{X}{T} \right) \right)^3 \exp \left(-Q^2 \gamma_Q \left(\frac{X}{T} \right) \right). \tag{23}$$

This function of X/T indeed resembles the early time density profile of the ROUP obtained by numerical simulations, with the characteristic 'valley' shape around the origin and maxima at $|X/T| = 2\sqrt{2}Q/3 \approx 0.943Q$, remarkably close to the numerically observed maxima situated at $0.948QT$ (see the above first section). It also tends very rapidly to zero as X/T tends towards $\pm Q$ because the Lorentz factor tends to infinity at these points, and the exponential thus tends to zero.

The above approximate expression for the short-time density profile can be recovered by reasoning directly on the phase-space density of the ROUP. Indeed, the Fourier transform $\hat{F}_Q$ of the phase-space density is, at early times, close to its initial value $F_Q^*/\sqrt{2\pi}$. As indicated above, $\mathcal{L}_Q F_Q^* = 0$. Thus, at early times, the Fourier transform $\hat{F}_Q$ obeys approximately (see Eq. (9))

$$\partial_T \hat{F} + iK\left(\frac{P}{\Gamma_Q(P)}\hat{F}\right) = 0, \qquad (24)$$

which can be integrated easily into:

$$\hat{F}_Q(T, K, P) \approx \frac{1}{\sqrt{2\pi}} F_Q^*(P) \exp\left(-i\frac{KP}{\Gamma_Q(P)}T\right). \qquad (25)$$

Carrying out the inverse Fourier transform and the integration over P delivers (23).

This analytical computation in *a priori* valid at short times only *i.e.* for values of T much smaller than unity. The numerical computations presented in the previous section extend well beyond $T \ll 1$. They reveal, in particular, that the density profile still presents the characteristic valley shape with peaks close to $0.94QT$ up to $T \approx 1$. The simulations are also useful in understanding how this valley shape transforms into the standard asymptotic Gaussian shape.

Let us finally note that the above analytical computation can be extended to other initial conditions and other models of finite-speed transport. This extension is presented in the Appendix to this article.
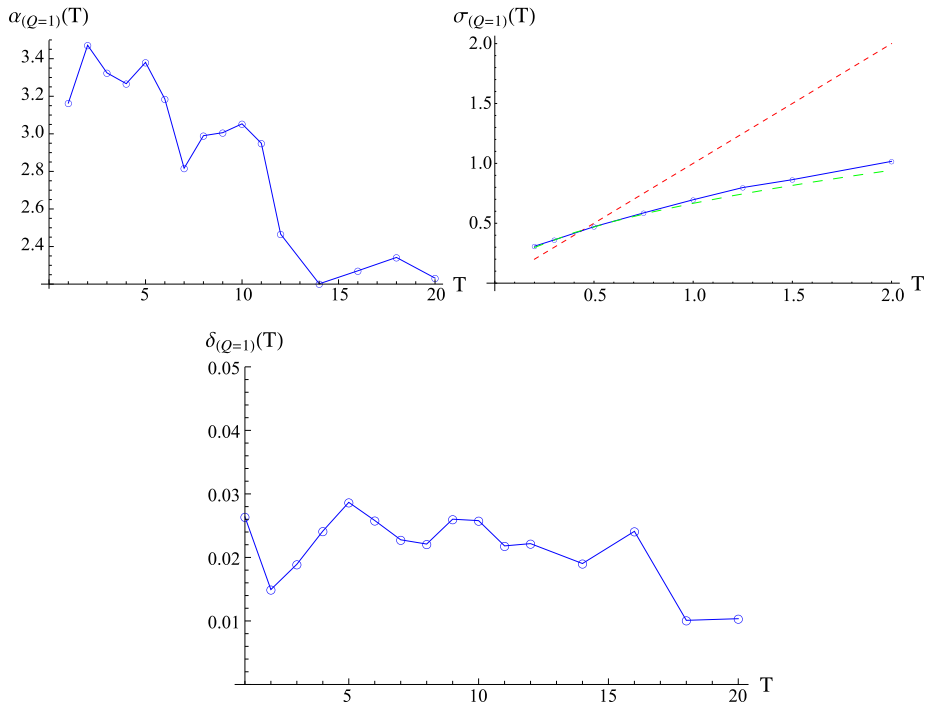
3.3 Fit of the Density Profile

Consider now the following function of position and time:

$$N_{\alpha,\sigma,B}(T, X) = B(T)\left(\gamma_Q\left(\frac{X}{T}\right)\right)^{\alpha(T)} \exp\left(-Q^2\gamma_Q\left(\frac{X}{T}\right)\right) \exp\left(-\frac{X^2}{2\sigma(T)^2}\right), \qquad (26)$$

where α and σ are two arbitrary functions of T and B ensures that $N_{\alpha,\sigma,B}$ is at all times normalized to unity on $(-QT, QT)$. At each time T, the values of $\alpha_Q(T)$, $\sigma_Q(T)$ and $B_Q(T)$ producing the best fits of N_Q can be obtained, for example, by minimizing the following distance function $d_C(T)$ between $N_Q(T, \cdot)$ and $N_{\alpha\sigma B}(T, \cdot)$:

$$d_C(T) = \int_{\mathbb{R}} \left|N_Q(T, X) - N_{\alpha\sigma B}(T, X)\right| dX + \lambda_B \left|1 - \int_{\mathbb{R}} N_{\alpha\sigma B}(T, X)\, dX\right|, \qquad (27)$$

where λ_B is a Lagrange multiplier which enforces normalization and the convention $N_{\alpha\sigma B}(T, X) = 0$ for $|X| > QT$ has been used. Figure 3 displays the results of the fit at different times for $Q = 1$ and $\lambda_B = 100$. The precision of the fit is always better than 3 % (see Fig. 3(bottom)). The coefficient α_Q remains close to the above computed value of 3 and seems to globally decrease with time; its average value for the points plotted in Fig. 3(top left) is 2.88. At small times, $\sigma_Q(T)$ behaves like $2\sqrt{T}/3$ (see the green

Fig. 3 Fit of the density profile. (*top left*) Time-evolution of the alpha-coefficient for $Q = 1$. (*top right*) Time-evolution of the σ-coefficient (*blue circles*) for $Q = 1$. The *straight line* is $x = ct$ *i.e.* $X = QT$ and the *dashed green curve* is $x = (2/3) \times \sqrt{k_B \theta_e t/(m\alpha^2)}$ *i.e.* $X = 2\sqrt{T}/3$. (*bottom*) Time-evolution of the absolute error of the fit for $Q = 1$

dashed curve on Fig. 3(top right)) and is thus larger than QT (the red straight line in Fig. 3(top right)); the Gaussian then varies slowly over $(-QT, +QT)$, the shape of the density profile is essentially controlled by the $\gamma_Q^{\alpha_Q(T)} \exp(-Q^2 \gamma_Q)$ and it thus displays the characteristic peaks at $|X/T|$ close to Q *i.e.* for x close to ct. As T increases, $\sigma_Q(T)$ becomes smaller than QT and the maximum of the Gaussian at $X = 0$ generates the secondary maximum at $X = 0$. As time still increases, $\sigma_Q(T)$ increases slowly from $2\sqrt{T}/3$ to $\sqrt{T}$ (the onset of this increase can actually be seen in Fig. 3(top right)) but $\sigma_Q(T)/QT$ continues to decrease towards zero; the density profile is then essentially controlled by the Gaussian and tends towards the standard result predicted by Fick's law.

Let us stress that the fit presented in this section is not based on an approximate analytical computation of the finite-time density profile, but is only a heuristic extension of the short-time computation presented in the previous section. This fit nevertheless highlights the fact that the whole time-evolution of the density profile can be understood in very simple terms *i.e.* as the superposition of two competing phenomena which are (i) the propagation of the peaks at velocity close to the light-velocity (ii) a standard Gaussian diffusion with a typical scaling as $\sqrt{T}$.

The fit also constitutes a simple, ready-to-use model of finite speed transport. It can be easily integrated into numerical simulations and should thus prove useful in a wide variety of physical and engineering applications.
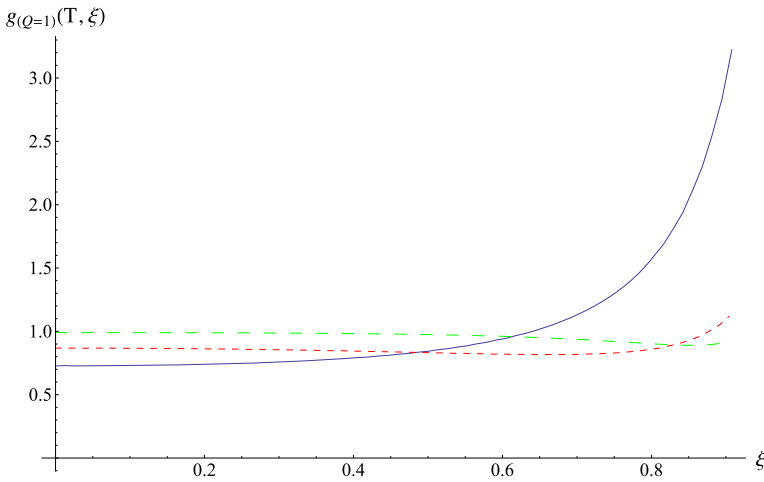
Fig. 4 Diffusion metric appearing in the generalized Fick's law. Metric g_Q plotted against the rescaled variable $\xi = x/(ct)$ for $Q = 1$ and $T = 1$ (*blue curve*), $T = 4$ (*red small dashes curve*), $T = 10$ (*green large dashes curve*)

4 Generalized Fick's Law

The generalized Fick's law obeyed by the ROUP is best understood in geometrical terms. Each Riemannian metric g defined over an n-dimensional physical space defines in a canonical manner a Brownian motion on this space. This result is well-known for time-independent metrics [28] but has been extended recently [2, 5–7, 9] to time-dependent ones. For this Brownian motion, the link between the density N (with respect to the g-independent measure dX), the current density J and the metric g reads

$$J(T, X) = \frac{1}{\sqrt{g(T, X)}} \partial_X \left(\frac{N(T, X)}{\sqrt{g(T, X)}} \right). \tag{28}$$

where $n = 1$ has been assumed. This last equation is a clear generalization of Fick's law. Changing point of view, this equation can also be viewed as a differential equation to be solved for the metric g at given density N and current J. Let g_Q be a metric thus associated to N_Q and J_Q. This metric is best obtained from N_Q and J_Q by rewriting (28) in terms of $h_Q = g_Q^{-1}$, which leads to:

$$\frac{N_Q}{2} \partial_X h_Q + h_Q \partial_X N_Q = -J_Q. \tag{29}$$

We choose as solution $h_Q(T, X) = I_Q(T, X)/N_Q^2(T, X)$ with

$$I_Q(T, X) = -2 \int_{-QT}^{X} N_Q(T, Y) J_Q(T, Y) \, dY. \tag{30}$$

The standard, Galilean Ornstein-Uhlenbeck process corresponds to $Q = +\infty$; as shown in [12], $J_\infty = -\chi(T)\partial_X N_\infty$, so that $h_\infty(T, X) = \chi(T)$, which is flat and tends (as it should) to 1, *i.e.* the time-independent Euclidean metric, as T tends to infinity.

Typical results are displayed in Fig. 4. The metric is nearly flat at the center of the interval $(-QT, QT)$ but grows to infinity near $|X| \sim QT$. Consider for example a point with

coordinate X and a point with coordinate $X + \Delta X$, $\delta X \ll X$. As far as the diffusion is concerned, the effective distance between these two points at time T is $g_Q(T, X) \Delta X$. This distance grows to infinity for any finite ΔX when X approaches $\pm QT$. Thus, the distance that a particle needs to travel to get closer to QT by the amount ΔX tends to infinity as the particle approaches $\pm QT$. This prevents the particle from ever crossing $X = \pm QT$ *i.e.* from being transported faster than light.

Let us add that the metric g_Q can be used to construct the space-time metric $\tilde{g}_Q$, defined by $ds^2 = dT^2 - g_Q(T, X) dX^2$, that $\tilde{g}_Q$ is conformal to $ds^2 = dT^2/\sqrt{g_Q(T, X)} - \sqrt{g_Q(T, X)} dX^2$, and that this last metric admits an horizon at $X = cT$.

We finally remark that the apparently simpler generalization of Fick's law $J = -D(T, X) \partial_X N$ is ruled out by numerical simulations (data not shown) because the current J_Q, in the short-time propagative regime, does not vanish at the two maxima of N_Q. A similar simple proportionality between J_Q and N_Q in Fourier space is also ruled out, for similar reasons.

5 Discussion

We have used the Relativistic Ornstein-Uhlenbeck Process to study the diffusion of relativistic particles in a fluid at equilibrium; to make the discussion definite, we have supposed that these particles start their stochastic motion from some arbitrary point O and that they are initially thermalized with the fluid. At short times, the density profile does not exhibit the standard spreading around O commonly associated to diffusion, but reveals propagation away from O at a velocity very close to the speed of light c. We have proposed a simple *Ansatz* which fits this profile at all times with a precision better than 3 %. We have also verified that the density profile of the ROUP does not obey Cattaneo's hyperbolic diffusion model, but a simple geometrical generalization of Fick's law. In physical space, the ROUP thus coincides with a Brownian motion in a time-dependent metric, and this metric tends with time towards the Euclidean metric.

The material presented in the Appendix presented suggests that all bounded velocity diffusions exhibit short-time propagative behavior, at least for a wide class of initial conditions. This could in principle be verified by direct experiments, at least for some Galilean diffusions. If short-time propagation is confirmed, the *Ansatz* (26) and the generalized Fick's law we propose in this article should be robust enough to accommodate most physically interesting situations.

The short-time propagation effect can be understood in rather simple, physical terms. Consider an arbitrary motion of a non-quantum point particle. At short times, the motion is entirely determined by the initial position and the initial velocity of the particle. If the initial velocity is distributed according to a certain probabilistic law, then the short-time motion of the particle is entirely determined by the initial position and the initial velocity law. This is true of all non-quantum motions and, in particular, of the physical diffusions of particles immersed in a fluid, whether the particles be relativistic or non-relativistic. Suppose now that a diffusing particle is initially in a thermal state of inverse temperature β. In both relativistic and non-relativistic cases, this state is represented by a Gibbs distribution [10, 17, 26] of the form $\exp(-\beta \epsilon(p)) dp$, where $\epsilon(p)$ is the energy of the particle. In the non-relativistic case, $\epsilon(p) = p^2/(2m)$ and $p = mv$. The initial velocity distribution is then Gaussian, it has no peak at non-vanishing velocities and there is thus no short-time propagation effect. In the relativistic case, $\epsilon(p) = mc^2\sqrt{1 + p^2/(mc)^2}$ and $v = p\epsilon(p)/c^2$. The direct computation presented in Sect. 3.2 and extended in the Appendix shows that the

corresponding velocity distribution presents two peaks at non-vanishing velocities $\pm\tilde{c}(\beta)$. Moreover, these are the only maxima of the velocity distribution provided the temperature is high enough (see the Appendix). In that case, the diffusing particle will undergo at short times a ballistic motion and essentially travel at velocities $\pm\tilde{c}(\beta)$. This is the propagation effect presented in this article. Naturally, as time increases, the cumulated effect of stochastic collisions becomes dominant and the propagation is replaced by standard diffusion. The simulations presented in this article show that, quite remarkably, the propagation effect is not short-lived *i.e.* is not restricted to infinitesimally short times, but that it extends at least to times of the same order as the inverse friction coefficient, which is the characteristic relaxation time of the system. The computation presented in the Appendix also shows that peaks in relativistic velocity distributions are encountered, not only in relativistic thermal states, but also in many other physically natural conditions, thus making short-time propagation a robust aspect of bounded velocity transport.

Let us stress that the metric generalizing the usual diffusion coefficient depends explicitly on the starting point O, on the time elapsed since the onset of diffusion, and on the initial temperature of the diffusing particles. All results presented in this article therefore admit non-trivial extensions to other, more general initial conditions. This should hopefully converge towards the obtention of a realistic and consistent hydrodynamical theory of special relativistic fluids, which has eluded physics since 1940 [17]. Galilean diffusions in an intrinsically curved space, like a membrane, and relativistic diffusions in space-times curved by gravity should also be investigated.

The generalized Fick's law points to a natural connection between bounded velocity diffusion and geometrical flows. A link with the geometry of black holes is also apparent. These connections will be explored in subsequent publications.

Appendix

Consider an arbitrary problem of finite speed transport and model it by a Langevin-type stochastic process. Restricting the discussion to 1D situations and using the same notations are in the core of the article, we write this process as:

$$dx = v\,dt \tag{31}$$

$$dv = F(v)dt + \sigma(v)dB_t \tag{32}$$

where F is a friction or dissipative term and σ is a noise coefficient. Since we are modeling finite speed transport, we suppose that the initial condition and the process itself restricts v to a finite interval, say $I = (-c, +c)$, where c is an arbitrary constant. A simple one-to-one map of this interval onto $\mathbb{R}$ is of course:

$$p : I \to \mathbb{R}$$
$$v \to p(v) = \gamma(v)\,v \tag{33}$$

with $\gamma(v) = (1 - \frac{v^2}{c^2})^{-1/2}$. Note that $v \to \pm c$ corresponds to $p \to \pm\infty$. The first equation of the process transcribes into

$$dx = \frac{p}{\Gamma(p)}\,dt \tag{34}$$

with $\Gamma(p) = (1 + p^2/c^2)^{1/2}$.

Consider now as initial condition $x = 0$ and a certain probability law in p, which we denote by $F^*(p)dp$. To make the discussion simpler, suppose also that F^* isotropic, and write $F^*(p) = \exp(-\Phi(\Gamma(p)))$. Reasoning as in Sect. 3.2 leads to the following approximate expression for the short-time density of the process in 1D space:

$$n(t,x) \approx \frac{1}{t}\left(\gamma\left(\frac{x}{t}\right)\right)^3 \exp\left(-\Phi\left(\gamma\left(\frac{x}{t}\right)\right)\right). \tag{35}$$

The first and second partial derivatives of n with respect to x read:

$$\frac{\partial n}{\partial x} = \frac{x}{c^2 t^2}\gamma^2\bigl(3 - \gamma\,\Phi'(\gamma)\bigr)n(t,x) \tag{36}$$

and

$$\frac{\partial^2 n}{\partial x^2} = \frac{\gamma^2}{c^2 t^2}\left[\bigl(3 - \gamma\,\Phi'(\gamma)\bigr)n + \frac{x^2}{c^2 t^2}\gamma\bigl(6\gamma - 3\gamma^2\Phi'(\gamma) - \gamma^3\Phi''(\gamma)\bigr)n \right.$$
$$\left. + x\bigl(3 - \gamma\Phi'(\gamma)\bigr)\frac{\partial n}{\partial x}\right]. \tag{37}$$

At early times, the density n thus admits an extremum at $x = 0$ *i.e.* for $\gamma = 1$. The second derivative of the density at $x = 0$ is non-negative provided $\Phi'(1) \le 3$ and $x = 0$ is then a local minimum of n. Suppose for example that $\Phi(\gamma) = a + q^2\gamma$. The initial momentum distribution is then a Jüttner distribution of temperature $k_B\theta_i = mc^2/q^2$ and $\Phi'(1) = q^2$. In this case, the origin $x = 0$ is a minimum for n at early times provided $q^2 \le 3$ or, equivalently, $k_B\theta_i \ge mc^2/\sqrt{3}$ *i.e.* for large enough initial temperatures. For initial temperatures smaller than $mc^2/\sqrt{3}$, $x = 0$ is a maximum for n. For these temperatures, the initial expectation or mean value $\bar{\gamma}$ of the Lorentz factor does not exceed ~ 1.2; the initial conditions for which $x = 0$ is a maximum of n are thus at most weakly relativistic.

Suppose now Φ is a strictly increasing function of γ and that the equation $\gamma\,\Phi'(\gamma) = 3$ has a single solution γ^*. This is so for $\Phi(\gamma) = a + q^2\gamma$, in which case $\gamma^* = 3/q^2$. At each time t, the value γ^* corresponds to $x/ct = \pm x^*/ct = \pm\sqrt{1 - 1/\gamma^{*2}}$. The second derivative of the density n at these points has the same sign as $D^* = -3\gamma^* - \gamma^{*3}\Phi''(\gamma^*)$. A sufficient (but not necessary) condition for D^* to be positive is that Φ be convex in γ. Thus, for any convex function Φ, the short-time density profile exhibits two peaks which travel at velocity $c\sqrt{1 - 1/\gamma^{*2}}$. For $\Phi(\gamma) = a + q^2\gamma$, a direct computation shows that the quotient $n(t, \pm x^*)/n(t, 0)$ is always greater or equal to unity and only reaches unity for $q = \sqrt{3}$. Thus, for this choice of Φ, the peaks are always higher than the extremum at $x = 0$, even when this extremum is a local maximum. The short-time transport is then always mainly propagative.

References

1. Angst, J., Franchi, J.: Central limit theorem for a class of relativistic diffusions. J. Math. Phys. **48**(8), (2007)
2. Arnaudon, M., Coulibaly, K.A., Thalmaier, A.: Brownian motion with respect to a metric depending on time. C. R. Acad. Sci. Paris **346**(13–14), 773–778 (2008)
3. Cattaneo, C.: Sulla conduzione del calore. Atti Semin. Mat. Fis. Univ. Modena **3** (1948)
4. Chen, H.T., Song, J.P., Liu, K.C.: Study of hyperbolic heat conduction problem in IC chip. Jpn. J. Appl. Phys. **43**(7A), 4404–4410 (2004)
5. Chevalier, C., Debbasch, F.: Multi-scale diffusion on an interface. Europhys. Lett. **77**, 20005 (2007)
6. Chevalier, C., Debbasch, F.: Is Brownian motion sensitive to geometry fluctuations? J. Stat. Phys. **131**, 717–731 (2008)

7. Chevalier, C., Debbasch, F.: Lateral diffusions: the influence of geometry fluctuations. Europhys. Lett. **89**(3), 38001 (2010)
8. Chevalier, C., Debbasch, F., Rivet, J.P.: A review of finite speed transport models. In: Proceedings of the Second International Forum on Heat Transfer (IFHT08), Sept. 17–19, 2008, Tokyo, Japan. Heat Transfer Society of Japan, Tokyo (2008)
9. Coulibaly-Pasquier, K.A.: Brownian motion with respect to time-changing Riemannian metrics. A. O. P. (2010, to appear)
10. Debbasch, F.: Equilibrium distribution function of a relativistic dilute prefect gas. Physica A **387**, 2443 (2008)
11. Debbasch, F., Rivet, J.P.: A diffusion equation from the relativistic Ornstein-Uhlenbeck process. J. Stat. Phys. **90**, 1179 (1998)
12. Debbasch, F., Rivet, J.P.: Time-dependent transport coefficients: an effective macroscopic description of small scale dynamics? C. R. Phys. Acad. Sci. **9**, 767–772 (2008)
13. Debbasch, F., Mallick, K., Rivet, J.P.: Relativistic Ornstein-Uhlenbeck process. J. Stat. Phys. **88**, 945 (1997)
14. Debbasch, F., Espaze, D., Foulonneau, V., Rivet, J.P.: Thermal relaxation for the Relativistic Ornstein-Uhlenbeck Process. Physica A **391**(15), 3797–3804 (2012)
15. Freidberg, J.: Plasma Physics and Fusion Energy. Cambridge University Press, Cambridge (2007)
16. Herrera, L., Pavon, D.: Why hyperbolic theories of dissipation cannot be ignored: comments on a paper by Kostadt and Liu. Phys. Rev. D **64**, 088503 (2001)
17. Israel, W.: Covariant fluid mechanics and thermodynamics: an introduction. In: Anile, A., Choquet-Bruhat, Y. (eds.) Relativistic Fluid Dynamics. Lecture Notes in Mathematics, vol. 1385. Springer, Berlin (1987)
18. Itina, T.E., Mamatkulov, M., Sentis, M.: Nonlinear fluence dependencies in femtosecond laser ablation of metals and dielectrics materials. Opt. Eng. **44**(5), 051109 (2005)
19. Jaunich, M.K., et al.: Bio-heat transfer analysis during short pulse laser irradiation of tissues. Int. J. Heat Mass Transf. **51**, 5511–5521 (2006)
20. Jüttner, F.: Das Maxwellsche Gesetz der Geschwindigkeitsverteilung in der Relativtheorie. Ann. Phys. (Leipz.) **34**, 856 (1911)
21. Kim, K., Guo, Z.: Multi-time-scale heat transfer modeling of turbid tissues exposed to short-pulse irradiations. Comput. Methods Programs Biomed. **86**(2), 112–123 (2007)
22. Klossika, J.J., Gratzke, U., Vicanek, M., Simon, G.: Importance of a finite speed of heat propagation in metal irradiated by femtosecond laser pulses. Phys. Rev. B **54**(15), 10277–10279 (1996)
23. Kumar, P., Narayan, R.: Grb 080319b: evidence for relativistic turbulence, not internal shocks. Mon. Not. R. Astron. Soc. **395**(1), 472–489 (2009)
24. Landau, L.D., Lifshitz, E.M.: The Classical Theory of Fields, 4th edn. Pergamon, Oxford (1975)
25. Martin-Solis, J.R., et al.: Enhanced production of runaway electrons during a disruptive termination of discharges heated with lower hybrid power in the Frascati Tokamak Upgrade. Phys. Rev. Lett. **97**, 165002 (2006)
26. Misner, C.W., Thorne, K.S., Wheeler, J.A.: Gravitation. Freeman, New York (1973)
27. Müller, I., Ruggeri, T.: Extended Thermodynamics. Springer Tracts in Natural Philosophy, vol. 37. Springer, New York (1993)
28. Øksendal, B.: Stochastic Differential Equations, 5th edn. Universitext. Springer, Berlin (1998)
29. Reif, F.: Fundamentals of Statistical and Thermal Physics. McGraw-Hill, Auckland (1965)
30. van Weert, Ch.: Some problems in relativistic hydrodynamics. In: Anile, A., Choquet-Bruhat, Y. (eds.) Relativistic Fluid Dynamics. Lecture Notes in Mathematics, vol. 1385. Springer, Berlin (1987)